Curr Radiol Rep (2018) 6:15
https://doi.org/10.1007/s40134-018-0272-x

NEUROIMAGING (T MASSOUD, SECTION EDITOR)

Imaging Parkinsonian Pathology in Substantia Nigra with MRI

Daniel E. Huddleston[1] · Jason Langley[2] · Petr Dusek[3,4] · Naying He[5] · Carlos C. Faraco[6] · Bruce Crosson[1,7,8] · Stewart Factor[1] · Xiaoping P. Hu[2,9]

Abstract

Purpose of Review The substantia nigra pars compacta (SNc) and its projection to the striatum undergo profound degeneration in Parkinson's disease (PD). Literature on imaging PD-related changes in the nigrostriatal system using iron-sensitive and diffusion-sensitive MRI contrasts has been contentious, with both negative and positive results reported in each contrast. These incompatible findings may be due to the inaccurate placement of regions of interest for the SNc.

Recent Findings Histologically, SNc is characterized by the presence of melanized dopamine neurons, whereas the substantia nigra pars reticulata is characterized by high iron content. Despite this histology, previous studies have frequently relied upon iron-sensitive MRI contrast when segmenting the SNc. This is also problematic since recent work found iron-sensitive and neuromelanin-sensitive contrasts are largely non-overlapping in substantia nigra. Since neuromelanin-sensitive MRI contrast colocalizes with the melanized dopamine neurons of the SNc upon radiologic–histologic correlation, the use of neuromelanin-sensitive MRI will allow for accurate localization of SNc and better capture parkinsonian pathobiology than iron-sensitive MRI.

Summary This article outlines iron-sensitive and diffusion-sensitive MRI contrasts, and provides an overview of neuromelanin-sensitive MRI techniques. The application of these techniques to image parkinsonian pathobiology in substantia nigra is then reviewed, with a focus on neuromelanin-sensitive imaging methods for the accurate and reproducible study of PD-related changes in SNc. These advances may help resolve current controversies surrounding MRI investigations of substantia nigra in PD and related disorders.

Keywords Neuromelanin · Substantia nigra · Parkinson's disease · Neuromelanin-sensitive MRI · Iron

This article is part of the Topical collection on *Neuroimaging*.

✉ Xiaoping P. Hu
xhu@engr.ucr.edu

1 Department of Neurology, Emory University, Atlanta, GA, USA

2 Center for Advanced Neuroimaging, University of California Riverside, Riverside, CA, USA

3 Department of Neurology and Center of Clinical Neuroscience, Charles University, 1st Faculty of Medicine and General University Hospital in Prague, Prague, Czech Republic

4 Department of Radiology, Charles University, 1st Faculty of Medicine and General University Hospital in Prague, Prague, Czech Republic

5 Department of Radiology, Ruijin Hospital, Shanghai Jiao Tong University School of Medicine, Shanghai, China

6 Department of Radiology and Radiological Science, Vanderbilt University Medical Center, Nashville, TN, USA

7 Department of Veterans Affairs Center for Visual and Neurocognitive Rehabilitation, Atlanta Veterans Affairs Medical Center, Decatur, GA, USA

8 Department of Psychology, Georgia State University, Atlanta, GA, USA

9 Department of Bioengineering, University of California Riverside, Materials Science and Engineering 205, Riverside, CA, USA

Published online: 20 March 2018

Introduction

Substantia nigra can be divided into two histologically and functionally distinct subregions, substantia nigra pars compacta (SNc) and substantia nigra pars reticulata (SNr). While both regions play prominent roles in cognitive and physiological processes, including reward based learning, novelty processing, and addiction [1–3], they have vastly different tissue compositions and connectivity profiles. Neurons in SNc project to posterior striatum, globus pallidus, prefrontal cortex, and anterior thalamus while the SNr neurons project to motor cortex and ventral anterior thalamus and receive projections from the striatum, external globus pallidus, and subthalamic nucleus [4, 5]. Compositionally, SNc is rich in neuromelanin-containing dopamine neurons, and contains lower concentrations of ferritin than SNr. The neurons of SNr are not melanized and produce the inhibitory neurotransmitter, gamma-aminobutyric acid, or GABA [6]. Together with the globus pallidus pars interna, the SNr is the main output nucleus of basal ganglia circuits [7, 8].

Neuromelanin is a complex pigment and byproduct of oxidative catabolism of catecholamines [9]. Neuromelanin comprised melanin, metal ions, lipids, and proteins. Melanins are able to bind large amounts of metals, presumably providing neuroprotection against their toxic properties [10, 11]. Among the metal ions, iron is the most abundant and neuromelanin has been shown to be the primary site for iron storage in pigmented neurons of the substantia nigra [12, 13]. Neuromelanin also sequesters potentially toxic catecholamine metabolites, and neuromelanin synthesis is driven by excess cytosolic catecholamines [14]. In substantia nigra, accumulation of neuromelanin begins around 3 years of age [15, 16] and neuromelanin concentration peaks around age 60 and decreases later in life [13, 17, 18]. Importantly, neuromelanin-containing neurons are not distributed evenly throughout SNc; instead, they are aggregated in clusters, referred to as nigrosomes [8].

Loss of neuromelanin-containing neurons in SNc, or depigmentation of SNc, is a primary macroscopic neuropathological characteristic of Parkinson's disease (PD), with much of the degeneration occurring prior to symptom onset [19, 20]. At the microscopic level, Lewy bodies, pathologic protein inclusions comprised predominantly aggregated alpha-synuclein, and neuromelanin-bound iron both accumulate in degenerating dopaminergic neurons [11, 21]. Extracellular neuromelanin released from dying neurons activates microglia and triggers a chronic inflammatory reaction in SNc. Neuronal loss is not uniform. It occurs first in caudal and lateral-ventral portions of the SNc, and then advances to more rostral portions as the disease progresses [22, 23]. Dopaminergic neurons in the lateral-ventral tier and caudal portions of SNc, i.e., the region containing the largest nigrosome (nigrosome 1), are the earliest and most profoundly affected in PD, as compared to dopaminergic neurons in other SNc subregions and to non-pigmented neurons [23, 24]. In addition, iron accumulation occurs in SNc concurrent with this neuronal loss and extensive evidence suggests that iron deposition is related to SNc neuronal loss and depigmentation [25–27]. Nigral iron deposits in PD are present predominantly in dystrophic microglial cells associated with extracellular neuromelanin and in the neuropil [28]. Furthermore, loss of neuromelanin-containing neuronal bodies is accompanied by axonal degeneration in the nigrostriatal pathway [29–32]. Taken together, in PD the SNc undergoes loss of pigmented neurons, extracellular release of neuromelanin from the dying neurons and associated microglial activation and iron accumulation [11]. Astrogliosis and local angiogenesis in SNc also occur in PD [33, 34].

Several imaging modalities can be used to visualize substantia nigra and nigrostriatal pathway in vivo: transcranial sonography (TCS), nuclear medicine techniques such as single-photon emission computed tomography (SPECT) or positron emission tomography (PET), and magnetic resonance imaging (MRI). While SPECT/PET imaging of nigrostriatal pathway integrity [35] and TCS detection of SN microstructural changes [36, 37] dominated the field of PD neuroimaging in the past decades, recent advances in MRI may be complementary or even advantageous to these methods. This article reviews quantitative MRI techniques utilizing contrasts sensitive to neuromelanin, iron, and microstructural tissue integrity and details their application in detecting PD-related changes in substantia nigra and the nigrostriatal pathway.

Imaging Substantia Nigra

Neuromelanin-Sensitive Techniques

Neuromelanin-sensitive MRI (NM-MRI) was introduced in 2006 by Sasaki, et al. [38]. Direct comparison of postmortem NM-MRI hyperintense signal with histology has found neuromelanin-containing neurons in locus coeruleus and SNc to colocalize with hyperintense signal in NM-MRI images [39••, 40]. Specifically, NM-MRI hyperintense signal in the brainstem anterior to the 4th ventricle has been localized to locus coeruleus [39••] and NM-MRI hyperintense signal in the mesencephalic tegmentum has been localized to SNc [40]. Similar results were obtained in a study on non-human primates comparing in vivo NM-MRI signal and postmortem SNc staining [41].

The original NM-MRI sequence relies on incidental magnetization transfer (MT) effects from an interleaved

multislice turbo spin-echo (TSE) sequence to generate neuromelanin-sensitive contrast [42]. This effect is illustrated in Fig. 1a where neuromelanin-sensitive contrast is observed in the multislice interleaved TSE acquisition (SNc appears as a hyperintense band in the brainstem). However, no neuromelanin-sensitive contrast is observed in either a single slice TSE or multislice sequential TSE acquisition (no MT effects are present in Fig. 1b or c). TSE-based NM-MRI delivers a high amount of radiofrequency energy [43, 44] and this deposition is a significant impediment to large-scale research and clinical application of TSE-based NM-MRI as it can lead to aborted scans or modified scan parameters.

Explicit MT effects can also be used to generate neuromelanin-sensitive contrast [40, 43–46]. Explicit MT generates neuromelanin-sensitive contrast by applying an off-resonance MT preparation pulse prior to excitation, and the necessity of MT preparation pulses to generate neuromelanin-sensitive contrast in SNc is illustrated in Fig. 2. MT prepared gradient recalled echo (GRE) two-dimensional [43] and three-dimensional [47, 48] pulse sequences have been developed to image SNc and LC. The GRE-based NM-MRI approach has several advantages over the TSE sequence: first, explicit MT effects are more controllable than incidental MT effects as incidental MT effects are dependent on the patient, echo train length, and repetition time; second, explicit MT effects provide better SNc and LC contrast than incidental MT effects from the TSE sequence [43]; third, GRE-based NM-MRI has been shown to deposit less radiofrequency energy (i.e., lower SAR) [43]. The exact mechanism of MT sensitivity to neuromelanin is not known. Interestingly, a recent in vitro study concluded that the primary mechanism underlying contrast in NM-MRI appears to be the T_1 reduction associated with melanin–iron complexes while the MT related to macromolecular neuromelanin content is not directly affected [46].

Iron-Sensitive Techniques

Substantia nigra has traditionally been imaged using T_2- or T_2*-weighted (T_2/T_2*-weighted) contrasts (see Fig. 3). A primary reason for the use of T_2/T_2*-weighted contrasts is that a subcomponent of substantia nigra, SNr, and a structure in its close proximity, red nucleus, contain elevated levels of iron relative to the surrounding brainstem. In T_2/T_2*-weighted images, both SNr and red nucleus appear as hypointense regions. This hypointensity is predominantly caused by paramagnetic effects from iron-containing ferritin [49], which induce local magnetic field inhomogeneities and increase R_2 ($R_2 = 1/T_2$) and R_2* ($R_2^* = 1/T_2^*$) relaxation rates. Transverse relaxation rates (R_2 or R_2*) can be measured by a multi-echo acquisition (spin echo and gradient echo for R_2 and R_2* measurements, respectively), then voxelwise fitting to an exponential model.

Paramagnetic effects from iron-containing proteins also increase bulk tissue magnetic susceptibility. These effects can be exploited using MR phase images to generate susceptibility-weighted contrast to better delineate structures with elevated paramagnetic iron species [50] or to measure the underlying susceptibility of tissue. Quantitative susceptibility mapping (QSM) measures relative susceptibility differences between tissues by modeling magnetic field inhomogeneities as magnetic dipoles, and then inverting this field to source susceptibility [51–53]. For subcortical structures with high iron content, such as SNr and red nucleus, there are large differences in susceptibility between these structures and the surrounding brainstem tissue, which can be used to clearly delineate these structures in vivo [54]. Studies have found that susceptibility

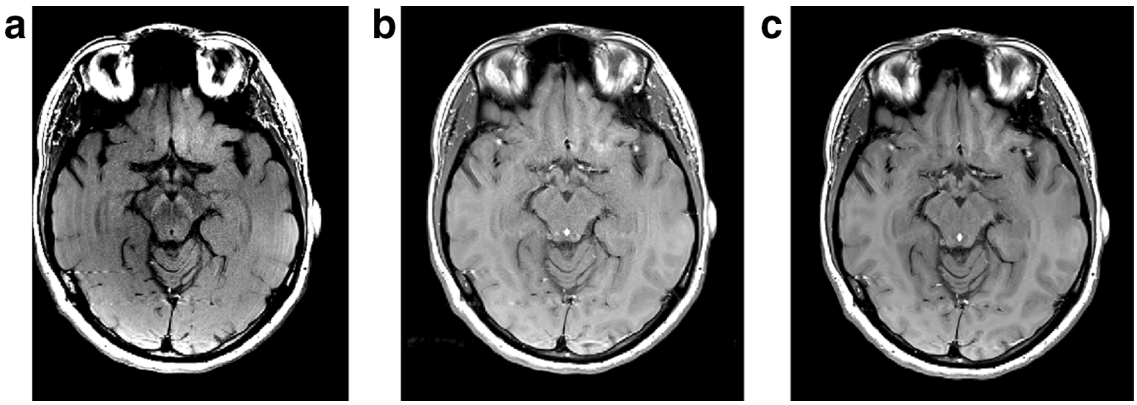

Fig. 1 Images from a multislice Sasaki TSE sequence [38] with interleaved acquisition (**a**) and sequential acquisition (**b**). An image of a single slice TSE acquisition is shown in (**c**). Only the multislice interleaved acquisition shows neuromelanin-sensitive contrast. Images were acquired at the Center for Advanced Neuroimaging at University of California Riverside

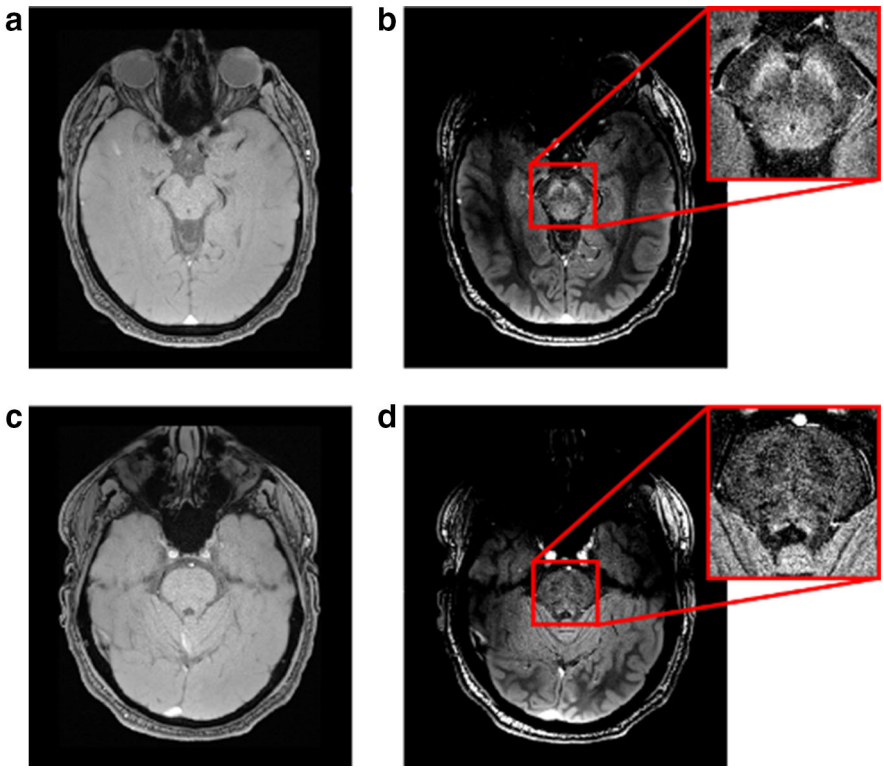

Fig. 2 Images from a gradient echo without (**a** and **c**) and with (**b** and **d**) magnetization preparation. Neuromelanin-sensitive contrast is observed in SNc and LC in **b** and **d**, respectively. Images were acquired using the NM-MRI parameters from Chen et al. [43] at the Center for Advanced Neuroimaging at University of California Riverside

values [55–57] and R_2 (or R_2*) values [58] correlate with iron concentration in the brain, but deep gray matter structures are more clearly delineated in QSM than in R_2* maps [52, 59].

Multi-contrast Imaging

The two subregions of substantia nigra, SNc and SNr, should exhibit different contrast profiles in NM-MRI and T_2/T_2*-weighted images given the differences in their composition [60]. Interestingly, comparison of substantia nigra in T_2/T_2*-weighted images and NM-MRI images found significant spatial discrepancy between the two substantia nigra volumes. The NM-MRI substantia nigra is located in a more caudal position as compared to the T_2*-weighted substantia nigra with approximately 10% overlap between the two substantia nigra volumes in healthy individuals [61]. This disparity is illustrated in Fig. 4.

Additional effort is needed to clarify the interpretation of neuromelanin-sensitive and iron-sensitive contrasts in substantia nigra. The differences in composition of SNc and SNr, coupled with the spatial inconsistency of NM-MRI and T_2/T_2*-weighted substantia nigra volumes, have led to the hypothesis that NM-MRI primarily images SNc while T_2/T_2*-weighted modalities are more sensitive to SNr [46, 61]. This hypothesis may explain the small overlap percentage between the two substantia nigra volumes, as histology found clusters of dopaminergic neurons from the SNc penetrate into the SNr [5]. In accordance with this observation, a hyperintense area within the lateral border of substantia nigra is consistently present surrounded by an iron-rich background on high-resolution T_2*-weighted MRI [62]. This area putatively corresponds to nigrosome-1, the largest cluster of pigmented neurons in substantia nigra [63, 64]. High-resolution ex vivo data also confirm blending of neuromelanin and iron contrasts (Fig. 5).

MRI–histological correlation studies examining the contrast profiles of SNc and SNr in NM-MRI and T_2/T_2*-weighted images are needed to verify the specificity of NM-MRI in the imaging of pigmented neurons. Further studies analyzing the structural and functional connectivity profiles of the NM-MRI defined SNc and T_2/T_2*-weighted substantia nigra may enhance our understanding of these substantia nigra volumes. In the remainder of the review, we will use SNc synonymously with the NM-MRI-defined substantia nigra and will use substantia nigra, or SNr, when the volume is derived from T_2/T_2*-weighted images.

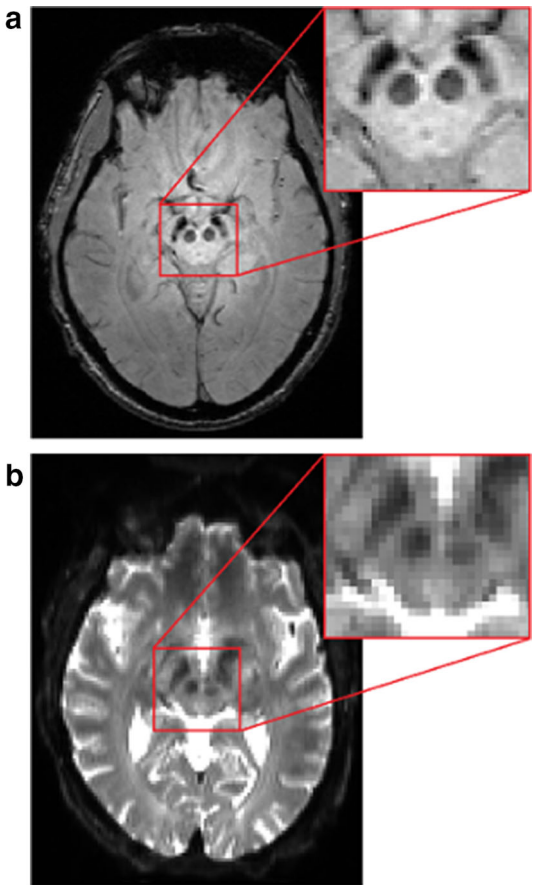

Fig. 3 Substantia nigra as seen in T_2/T_2*-weighted images. The substantia nigra in a gradient-echo image (T_2*-weighted) and a spin-echo EPI (T_2-weighted) are shown in a and b, respectively. In both images, red nucleus is defined as the bilateral circles in the brain stem and substantia nigra is the hypointense band lateral to red nucleus. Images were acquired at Emory University using parameters from [97] and [109]

Parkinsonian Pathology in Substantia Nigra

Neuromelanin-Related Parkinsonian Pathophysiology

Colocalization of neuromelanin-sensitive contrast with anatomic structures containing neuromelanin has led to the increasing use of NM-MRI to study locus coeruleus and/or the SNc in vivo in parkinsonian disorders. Most clinical NM-MRI studies have used the Sasaki TSE sequence to generate neuromelanin-sensitive contrast and, to date, relatively few studies used explicit magnetization transfer effects to generate neuromelanin-sensitive contrast. The TSE-based approach has been applied to find reduced contrast ratios in locus coeruleus or SNc in PD patients as compared to controls [38, 65, 66], or reductions in SNc volume of PD patients [67]. Other work has found a reduction in SNc area of a single slice [44, 68] or SNc volume [69, 70] of PD patients using the TSE-based approach. Lower SNc volume was observed in PD patients using the GRE-based approach [47, 71].

NM-MRI has been used as a tool for differential diagnosis of essential tremor, multiple system atrophy (MSA), or progressive supranuclear palsy (PSP) versus PD. Reductions in SNc area of PD patients were observed, but no differences in SNc area were seen between essential tremor and controls [72]. In [73], MSA, PSP, and PD groups exhibited lower SNc volume as compared to controls but no difference in SNc volume was observed between MSA, PSP, or PD groups. The inability to distinguish PD and MSA has also been reported by Ohtsuka et al. [74]. Another report examined contrast ratios in locus coeruleus and SNc of PD patients, Alzheimer's disease patients, and healthy subjects and found reduced contrast ratios in locus coeruleus and SNc of early and late stage PD patients as compared to healthy subjects, but no change in locus coeruleus contrast ratio or SNc in Alzheimer's disease patients was observed [75].

Iron-Related Parkinsonian Pathophysiology

In PD, iron deposition occurs concurrently with neuromelanin depletion in SNc [25, 26, 76], and given the relationship between iron and SNc depigmentation, many studies have examined substantia nigra iron deposition in parkinsonian disorders using transverse relaxation rate (R_2 or R_2*) mapping [49, 71, 77–88], susceptibility-weighted imaging (SWI) [89–91], or QSM [54, 92–94] techniques. There is no clear consensus in regard to iron deposition as

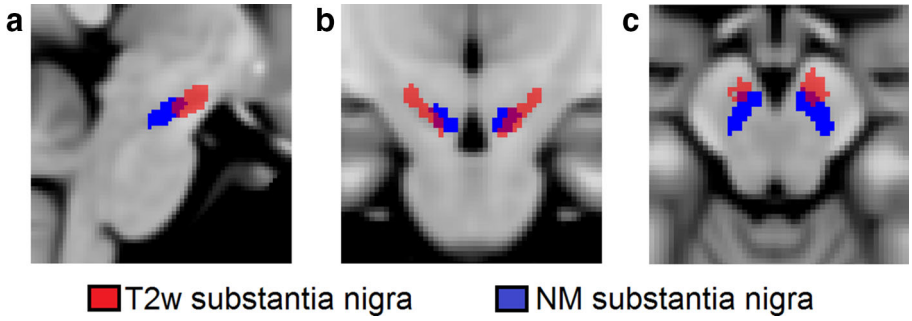

Fig. 4 Comparison of NM-MRI (blue) and T_2-weighted (red) substantia nigra volumes. The two substantia nigra volumes are nearly spatially disjoint with approximately 10% overlap between the two volumes

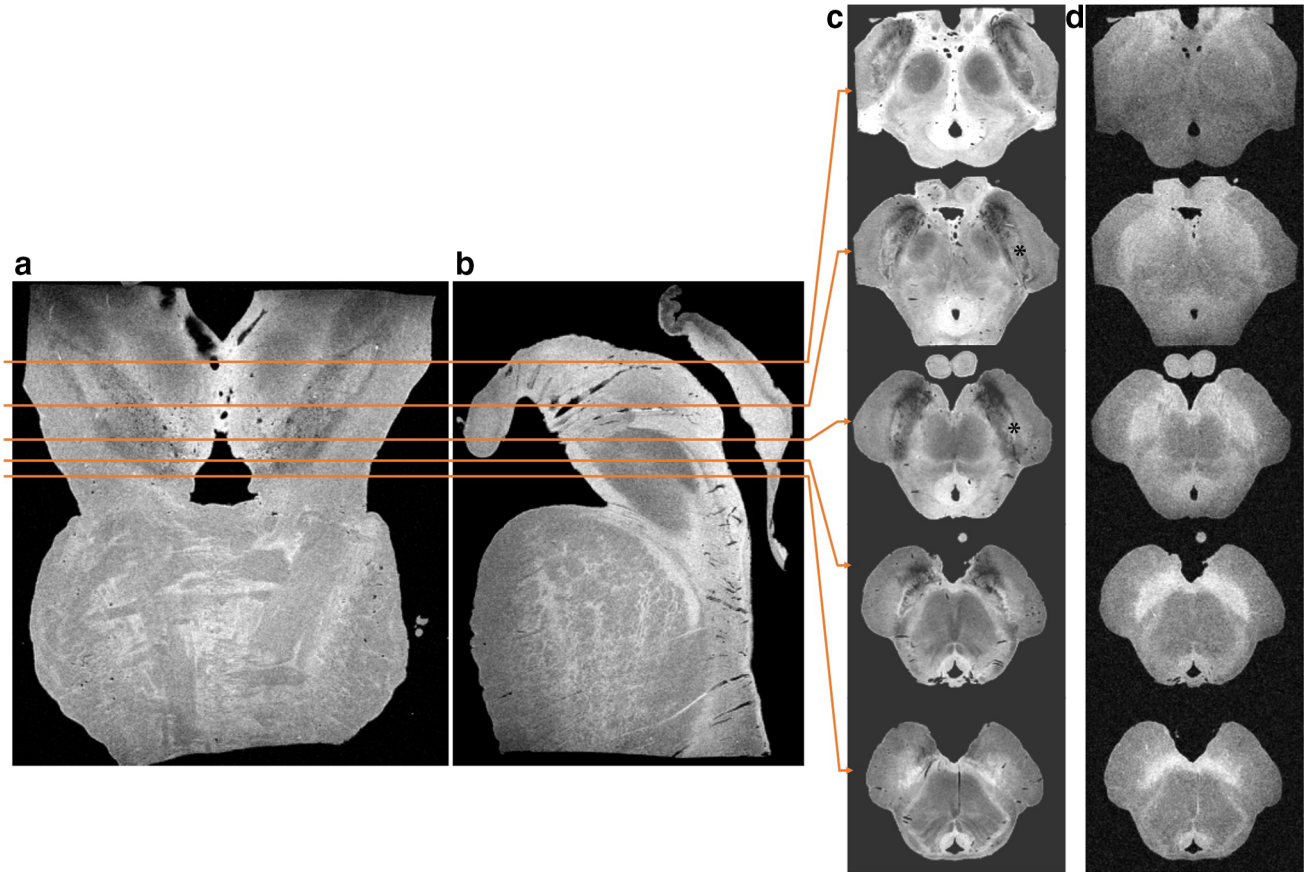

Fig. 5 Iron-sensitive and neuromelanin-sensitive contrasts at various levels of substantia nigra. High-resolution (voxel size = 200 mm^3 isotropic) scans of normal postmortem brainstem are shown whereby lines on coronal (**a**) and sagittal (**b**) sections denote positions of axial slices in columns c (iron-sensitive MRI) and d (NM-MRI). Iron contrast dominates in the cranial and medial part, while neuromelanin contrast dominates in caudal and medial part of substantia nigra. predominantly within lateral aspects of substantia nigra on iron-sensitive MRI (**c**) are supposedly representing clusters of neuromelanin-containing neurons. In (**c**), nigrosome 1 is labeled with a * on the right side but is not labeled on the left side to improve visualization of substantia nigra structure. Images were acquired at B.U.F.F., Max Delbrueck Center for Molecular Medicine, Berlin, Germany using 9.4T Bruker animal scanner. Images were scanned at room temperature with the following parameters for each contrast: Iron-sensitive: 3D-GRE, TR = 40 ms, FA = 40°, NEX = 8, 5 equidistant echoes TEs = 3.4–23.4 ms were averaged to generate the image; NM sensitive: 3D-GRE, TR = 20 ms, FA = 15°, TE = 1.6 ms, NEX = 15 (MT pulse: duration = 2 × 3 ms, FA = 913°, frequency offset = 800 Hz)

measured with iron-sensitive MRI contrasts. Increases in transverse relaxation rate [49, 77–83, 95] or susceptibility values [54, 92] in substantia nigra of PD patients have been reported but other studies have observed no differences in substantia nigra transverse relaxation rates [71, 84–88] or susceptibility values [71].

This disagreement may be due to differences in the definition of regions of interest (ROIs) for SNc and SNr among studies evaluating iron deposition in PD [78, 81, 96]. ROIs used in the aforementioned analyses were defined using T_2/T_2*-weighted images, which are not sensitive to neuromelanin [61]. In most iron mapping studies, the substantia nigra was defined as the hypointense region between the red nucleus and cerebral peduncle. The substantia nigra derived from this definition is spatially incongruent with the substantia nigra as seen in NM-MRI images [61]. Since NM-MRI signal colocalizes with SNc [40], and the SNr is iron-rich, the ROIs for SNc placed in the T_2/T_2*-weighted, SWI, or QSM contrast region of substantia nigra most likely inadvertently selected SNr and largely excluded SNc [97]. The use of NM-MRI to define SNc ROIs may improve consistency in studies analyzing iron deposition in SNc.

There are a few recent studies analyzing iron deposition in the NM-MRI-defined SNc. One study found increased nigral hypointensity in T_2-weighted images in the lateral-ventral tier of the neuromelanin-defined SNc in PD patients as compared to controls [97]. In a different study [98•], regions undergoing this deposition were found to exhibit decreased neuromelanin-sensitive contrast. Both results appear to be consistent with histopathology findings of selective loss of melanized dopamine neurons in the

lateral-ventral SNc in PD, first observed by Hassler in 1938 and subsequently replicated by multiple groups [22, 23, 99, 100]. This subregion contains the largest nigrosome, nigrosome-1. Interestingly, these findings support the theory that loss of lateral-ventral SNc NM-MRI hyperintensity and an increase in lateral-ventral SNc T_2-weighted hypointensity represent neuromelanin loss and iron accumulation in nigrosome-1 in PD.

Nigrosome-1 can be seen as a hyperintense region in the substantia nigra of T_2/T_2*-weighted images resembling a 'swallow tail' [101]. In PD, a lack of hyperintensity is reliably observed in this region at 3T [63, 102–104] and higher magnetic field strengths [105]. Figure 6 shows an ex vivo comparison of nigrosome 1 between a PD subject and a healthy control subject. Other groups have studied nigrosome-1 with iron-sensitive MRI contrasts and identified PD effects as well, although they discuss this finding as "loss of dorsolateral nigral hyperintensity" [103]. This reflects anatomic orientation from the perspective T_2/T_2* contrast in substantia nigra. The loss of hyperintensity in T_2/T_2* images in this region represents iron deposition occurring in the lateral-ventral SNc, although these studies did not use a NM-MRI population mask to define SNc. But, overall, these results indicate that lateral-ventral SNc/nigrosome-1 imaging is a promising approach for PD diagnostic biomarker development [103]. Another study found the width of the middle slice of SNc was reduced in PD but no increase in iron was observed [106]. ROIs in [106] were placed in neuromelanin-sensitive and T_2*-weighted images separately and, given the spatial discord between substantia nigra in T_2*-weighted and neuromelanin-sensitive images, may not have been placed in the same location.

Substantia Nigra Microstructure

Diffusion-weighted imaging (DWI) and diffusion tensor imaging (DTI) allow for the assessment of tissue microstructure by examining the diffusion of water molecules in the brain. DTI is able to measure tissue microstructure by examining diffusion restriction and anisotropy between intracellular and extracellular compartments. Tissue microstructure is most often assessed using fractional anisotropy (FA), a measure related to fiber bundle cohesion, or mean diffusivity (MD), a measure of the extent of diffusion, or radial diffusivity (RD), a measure of diffusivity perpendicular to fiber bundles.

PD-related SNc neuronal loss should remove barriers to diffusion, thereby increasing MD, and increase diffusion dispersion, reducing FA. This selective loss, largely confined to SNc, has been used to differentiate PD from MSA and PSP, where more widespread neurodegenerative changes occur [107, 108]. However, results regarding PD-related changes in substantia nigra are inconclusive with several DTI studies finding lower FA in substantia nigra of PD [78, 82, 109–111], increased FA in substantia nigra [112], or no difference in FA substantia nigra [84, 85, 113–115]. Variability of substantia nigra ROIs used in each study may account for inconsistent results of these studies [114]. ROIs used in the aforementioned DTI studies, excluding [109] which used NM-MRI to define SNc ROIs, were defined using T_2-weighted $b = 0$ images and, given the spatial discrepancy between substantia nigra seen in T_2-weighted and neuromelanin-sensitive images [61], may be located outside SNc. Thus, inconsistencies in SNc DTI metrics across studies may be attributed to improper ROI placement. The paramagnetic effects of iron on the DTI metrics may have contributed to inconsistent results as well [116].

Alternatively, the lack of accord in studies examining substantia nigra with the standard DTI model may be due to the simplicity of the standard DTI model. More sophisticated models of diffusion, such as free water imaging or neurite orientation dispersion and density imaging (NODDI), account for tissue microstructure by

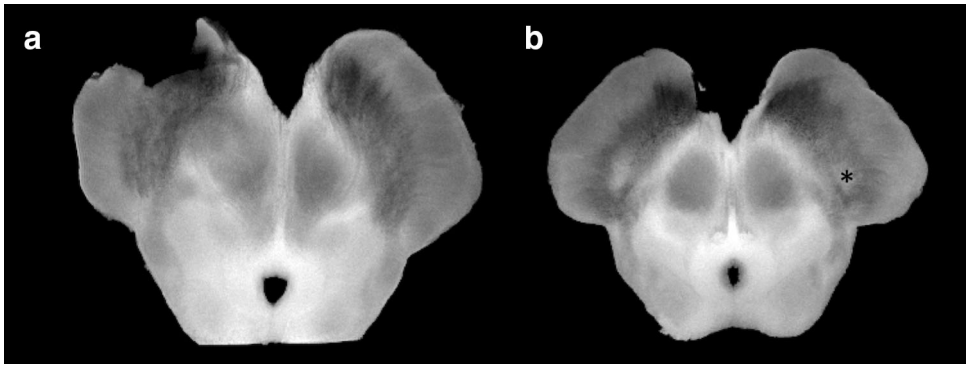

Fig. 6 *Ex vivo* T_2-weighted MRI images of the mid-mesencephalon in a PD patient (**a**) and healthy control (**b**). Nigrosome-1, marked as * on the right side of (**b**) is seen in the healthy control but is absent in the PD. Nigrosome-1 on the left side of (**b**) was not marked to improve visualization. The images in (**a**) and (**b**) are averaged over 20 slices of the mid-mesencephalon and imaging parameters used to acquire the data are listed in Fig. 5

directly incorporating the intracellular and extracellular compartments in the diffusion model. Other diffusion models, such as diffusion kurtosis imaging (DKI), account for the non-Gaussianity of diffusion in tissue. These sophisticated diffusion models may better capture microstructural changes in substantia nigra from parkinsonian disorders and have found changes in substantia nigra as defined in T_2-weighted images [30, 112, 117, 118].

In addition to the aforementioned studies examining substantia nigra microstructure, DTI tractography can be used to probe the integrity of the nigrostriatal tract or to identify SNc and SNr. Reduced connectivity has been observed between substantia nigra, defined with T_1 maps [113] or T_2/T_2*-weighted images [119, 120], to the striatum of PD patients. Other work found reduced FA in the nigrostriatal tract [121] or correlations between a measure of motor dysfunction, Unified Parkinson's Disease Rating Scale (UPDRS) [122] scores, and FA in the nigrostriatal tract [123]. Interestingly, DTI tractography has been applied to parcellate SNc and SNr in substantia nigra volumes segmented from T_1 maps [124]. The relative locations SNc and SNr from this study align with the location of substantia nigra seen in NM-MRI and T_2*-weighted contrasts, respectively [61].

Conclusions and Perspectives

The ability to detect parkinsonian biopathology has been improved by recent advances in imaging iron, tissue microstructure, and neuromelanin. These advancements may allow the timing of PD-related changes to be ascertained or develop new biomarkers for early detection of PD. However, additional work is needed to resolve the inconsistent results seen in SNc in PD studies using iron-sensitive and diffusion MRI contrasts. Consistency in SNc ROI selection using standard space ROIs may improve reproducibility of studies. Further, more accurate phenotyping of PD subjects may increase agreement across studies.

ROI selection for substantia nigra in studies examining iron deposition or microstructural changes is typically done using T_2- or T_2*-weighted images. The application of SNc ROIs from NM-MRI to iron-sensitive and diffusion MRI contrasts should be done with caution since significant degeneration in SNc will have occurred at the time of PD diagnosis [19, 20]. This degeneration will be present as either a reduction of neuromelanin-sensitive contrast or volume in subject-specific NM-MRI SNc volumes. Thus, regions most affected by PD may not be included in NM-MRI SNc of PD patients. However, these regions will still be present in control NM-MRI SNc ROIs, and the use of control SNc ROIs will allow for the inspection of SNc regions already affected by PD [97].

Clinical PD is a heterogeneous disorder with several overlapping phenotypes defined clinically, genetically, or using various biomarkers [125–128]. Degeneration of the nigrostriatal pathway is shared by all PD phenotypes, but the different phenotypes may affect the nigrostriatal pathway and other brain systems differently. The tremor-dominant PD phenotype has a slower progression than the akinetic-rigid PD phenotype and there is milder loss of dopaminergic neurons in the tremor-dominant phenotype [129]. The tremor-dominant PD phenotype is thought to interrupt the cerebellothalamocortical circuit and impairment of striatothalamocortical circuits is a hallmark of the akinetic-rigid PD phenotype [130–132]. The tremor-dominant PD phenotype is therefore expected to be associated with damage to structures in the cerebellothalamocortical circuit, such as the dentate nucleus. A recent study examined structural changes in tremor-dominant and akinetic-rigid phenotypes and found increased iron deposition in dentate nucleus of tremor-dominant PD subjects as compared to control and akinetic-rigid PD subjects [133]. It was speculated that oxidative stress from this deposition may lead to neuronal loss in the dentate nucleus, disrupt functional connectivity in cerebellothalamocortical circuit, and cause tremor [133].

Improved subject phenotyping coupled with consistent SNc ROI selection may allow causality of SNc neuronal loss and SNc iron deposition to be determined. These changes have been observed in histology but the causality of these changes is in contention with a portion of the literature suggesting iron deposition is a byproduct of SNc degeneration and associated neuroinflammatory changes [134, 135] and another portion suggesting that iron deposition and dysregulation of its homeostasis drive SNc neuronal loss [136, 137]. Knowledge of the causality of these changes is crucial for the development of prodromal biomarkers of PD and enable clinical trials of potential PD interventions. For example, if neuronal loss is driven by iron deposition then changes in susceptibility and R_2* may be observed in the NM-MRI-defined SNc, while if iron deposition is a byproduct of neuronal loss then SNc volume loss should occur prior to changes in measures of iron deposition.

In addition to determining the causality of changes in SNc, MRI can be used to examine the pathologic progression of PD. The leading hypothesis for pathologic progression of PD, the Braak Hypothesis, stipulates that locus coeruleus exhibits Lewy pathology at an earlier stage (Braak Stage 2) than SNc (Braak Stage 3) [138]. Other histopathologic work has reported that neuronal loss is more profound in locus coeruleus than SNc in PD [139]. In the context of the Braak Hypothesis it has been suggested

that many non-motor symptoms of PD, which often precede onset of motor symptoms, may be attributable to the degeneration of nuclei in lower brainstem, namely locus coeruleus. These include mood, cognitive, and sleep changes [140]. However, due to a lack of adequate tools, there has been no convincing investigation of the Braak Hypothesis in vivo, and the hypothesis remains controversial [141, 142]. Identification and verification of an ascending sequential degeneration of brainstem catecholamine nuclei in PD in living patients would serve to address this controversy. NM-MRI is well poised to examine the Braak Hypothesis in vivo since the method has been shown to exhibit reproducible neuromelanin-sensitive contrast and volume in SNc and locus coeruleus has been shown to be repeatable in separate scans [143]. Another possible application of NM-MRI is its use as a diagnostic tool and marker of SNc degeneration in PD, complementing existing nuclear medicine techniques. NM-MRI and dopamine transporter SPECT/PET of the nigrostriatal projection show prominent pathology in PD, suggesting that both methods are sensitive to PD-related nigrostriatal degeneration [144]. In support of this, a pilot study comparing NM-MRI and dopamine transporter SPECT found a good correlation between these methods [145].

In summary, multimodal studies utilizing a combination of neuromelanin-sensitive, iron-sensitive, and diffusion contrasts are well poised to comprehensively examine parkinsonian-related changes in substantia nigra. Incorporation of NM-MRI in imaging studies examining iron deposition or microstructural changes will allow for greater understanding of the changes occurring in SNc in PD. Specifically, multi-contrast studies involving NM-MRI and other MRI contrasts may be used to examine causal relationships between iron deposition and neuronal loss in SNc. Finally, NM-MRI may provide insight into the pathologic progression of PD and verify or refute the Braak hypothesis.

Acknowledgements Xiaoping Hu and Daniel E. Huddleston receive support from the Michael J. Fox Foundation (MJF 10854). Petr Dusek is supported by Czech Science Foundation (grant nr. 16-07879S) and Czech Ministry of Health (grant nr. 15-25602A). Bruce Crosson receives support from the Rehabilitation Research & Development Service of the Department of Veterans Affairs Office of Research and Development (award nr. B6364-L).

Compliance with Ethical Guidelines

Conflict of interest Daniel E. Huddleston, Jason Langley, Petr Dusek, Naying He, Carlos C. Faraco, Bruce Crosson, Stewart Factor, and Xiaoping Hu each declare no potential conflicts of interest.

Human and Animal Rights and Informed Consent This article does not contain any studies with human or animal subjects performed by any of the authors.

References

Recently published papers of particular interest have been highlighted as:
- • Of importance
- •• Of major importance

1. Guitart-Masip M, Huys QJ, Fuentemilla L, Dayan P, Duzel E, Dolan RJ. Go and no-go learning in reward and punishment: interactions between affect and effect. NeuroImage. 2012;62(1):154–66.
2. Kimura K, Hikida T, Yawata S, Yamaguchi T, Nakanishi S. Pathway-specific engagement of ephrinA5-EphA4/EphA5 system of the substantia nigra pars reticulata in cocaine-induced responses. Proc Natl Acad Sci USA. 2011;108(24):9981–6.
3. Schiffer AM, Ahlheim C, Wurm MF, Schubotz RI. Surprised at all the entropy: hippocampal, caudate and midbrain contributions to learning from prediction errors. PLoS ONE. 2012;7(5):e36445.
4. Beckstead RM, Domesick VB, Nauta WJ. Efferent connections of the substantia nigra and ventral tegmental area in the rat. Brain Res. 1979;175(2):191–217.
5. Haber SN. The primate basal ganglia: parallel and integrative networks. J Chem Neuroanat. 2003;26(4):317–30.
6. Atherton JF, Bevan MD. Ionic mechanisms underlying autonomous action potential generation in the somata and dendrites of GABAergic substantia nigra pars reticulata neurons in vitro. J Neurosci. 2005;25(36):8272–81.
7. Snyder AM, Connor JR. Iron, the substantia nigra and related neurological disorders. Biochim Biophys Acta. 2009;1790(7):606–14.
8. Damier P, Hirsch EC, Agid Y, Graybiel AM. The substantia nigra of the human brain. I. Nigrosomes and the nigral matrix, a compartmental organization based on calbindin D(28 K) immunohistochemistry. Brain. 1999;122(Pt 8):1421–36.
9. Graham DG. Oxidative pathways for catecholamines in the genesis of neuromelanin and cytotoxic quinones. Mol Pharmacol. 1978;14(4):633–43.
10. Zecca L, Casella L, Albertini A, Bellei C, Zucca FA, Engelen M, et al. Neuromelanin can protect against iron-mediated oxidative damage in system modeling iron overload of brain aging and Parkinson's disease. J Neurochem. 2008;106(4):1866–75.
11. Zucca FA, Segura-Aguilar J, Ferrari E, Munoz P, Paris I, Sulzer D, et al. Interactions of iron, dopamine and neuromelanin pathways in brain aging and Parkinson's disease. Prog Neurobiol. 2017;155:96–119.
12. Zecca L, Gallorini M, SchuÈnemann V, Trautwein AX, Gerlach M, Riederer P, et al. Iron, neuromelanin and ferritin content in the substantia nigra of normal subjects at different ages: consequences for iron storage and neurodegenerative processes. J Neurochem. 2001;76(6):1766–73.
13. Zecca L, Stroppolo A, Gatti A, Tampellini D, Toscani M, Gallorini M, et al. The role of iron and copper molecules in the neuronal vulnerability of locus coeruleus and substantia nigra during aging. Proc Natl Acad Sci USA. 2004;101(26):9843–8.
14. Sulzer D, Bogulavsky J, Larsen KE, Behr G, Karatekin E, Kleinman MH, et al. Neuromelanin biosynthesis is driven by excess cytosolic catecholamines not accumulated by synaptic vesicles. Proc Natl Acad Sci USA. 2000;97(22):11869–74.
15. Fenichel GM, Bazelon M. Studies on neuromelanin. II. Melanin in the brainstems of infants and children. Neurology. 1968;18(8):817–20.

16. Cowen D. The melanoneurons of the human cerebellum (nucleus pigmentosus cerebellaris) and homologues in the monkey. J Neuropathol Exp Neurol. 1986;45(3):205–21.
17. Ma SY, Roytt M, Collan Y, Rinne JO. Unbiased morphometrical measurements show loss of pigmented nigral neurones with ageing. Neuropathol Appl Neurobiol. 1999;25(5):394–9.
18. Manaye KF, McIntire DD, Mann DM, German DC. Locus coeruleus cell loss in the aging human brain: a non-random process. J Comp Neurol. 1995;358(1):79–87.
19. Riederer P, Wuketich S. Time course of nigrostriatal degeneration in parkinson's disease. A detailed study of influential factors in human brain amine analysis. J Neural Transm. 1976;38(3–4):277–301.
20. Halliday GM, McRitchie DA, Cartwright H, Pamphlett R, Hely MA, Morris JG. Midbrain neuropathology in idiopathic Parkinson's disease and diffuse Lewy body disease. J Clin Neurosci. 1996;3(1):52–60.
21. Mosharov EV, Larsen KE, Kanter E, Phillips KA, Wilson K, Schmitz Y, et al. Interplay between cytosolic dopamine, calcium, and alpha-synuclein causes selective death of substantia nigra neurons. Neuron. 2009;62(2):218–29.
22. Damier P, Hirsch EC, Agid Y, Graybiel AM. The substantia nigra of the human brain. II. Patterns of loss of dopamine-containing neurons in Parkinson's disease. Brain. 1999;122(Pt 8):1437–48.
23. Fearnley JM, Lees AJ. Ageing and Parkinson's disease: substantia nigra regional selectivity. Brain. 1991;114(Pt 5):2283–301.
24. Hirsch E, Graybiel AM, Agid YA. Melanized dopaminergic neurons are differentially susceptible to degeneration in Parkinson's disease. Nature. 1988;334(6180):345–8.
25. Dexter DT, Carayon A, Javoy-Agid F, Agid Y, Wells FR, Daniel SE, et al. Alterations in the levels of iron, ferritin and other trace metals in Parkinson's disease and other neurodegenerative diseases affecting the basal ganglia. Brain. 1991;114(Pt 4):1953–75.
26. Dexter DT, Wells FR, Agid F, Agid Y, Lees AJ, Jenner P, et al. Increased nigral iron content in postmortem parkinsonian brain. Lancet. 1987;2(8569):1219–20.
27. Witoszynskyj S, Rauscher A, Reichenbach JR, Barth M. Phase unwrapping of MR images using Phi UN–a fast and robust region growing algorithm. Med Image Anal. 2009;13(2):257–68.
28. Morris CM, Edwardson JA. Iron histochemistry of the substantia nigra in Parkinson's disease. Neurodegeneration. 1994;3(4):277–82.
29. Zucca FA, Segura-Aguilar J, Ferrari E, Munoz P, Paris I, Sulzer D, et al. Interactions of iron, dopamine and neuromelanin pathways in brain aging and Parkinson's disease. Prog Neurobiol. 2015;155:96–119.
30. Planetta PJ, Ofori E, Pasternak O, Burciu RG, Shukla P, DeSimone JC, et al. Free-water imaging in Parkinson's disease and atypical parkinsonism. Brain. 2016;139(Pt 2):495–508.
31. Urrutia PJ, Mena NP, Nunez MT. The interplay between iron accumulation, mitochondrial dysfunction, and inflammation during the execution step of neurodegenerative disorders. Front Pharmacol. 2014;5:38.
32. Walsh S, Finn DP, Dowd E. Time-course of nigrostriatal neurodegeneration and neuroinflammation in the 6-hydroxydopamine-induced axonal and terminal lesion models of Parkinson's disease in the rat. Neuroscience. 2011;175:251–61.
33. Faucheux BA, Bonnet AM, Agid Y, Hirsch EC. Blood vessels change in the mesencephalon of patients with Parkinson's disease. Lancet. 1999;353(9157):981–2.
34. Desai Bradaric B, Patel A, Schneider JA, Carvey PM, Hendey B. Evidence for angiogenesis in Parkinson's disease, incidental Lewy body disease, and progressive supranuclear palsy. J Neural Transm. 2012;119(1):59–71.
35. Strafella AP, Bohnen NI, Perlmutter JS, Eidelberg D, Pavese N, Van Eimeren T, et al. Molecular imaging to track Parkinson's disease and atypical parkinsonisms: new imaging frontiers. Mov Disord. 2017;32(2):181–92.
36. Walter U. Transcranial brain sonography findings in Parkinson's disease: implications for pathogenesis, early diagnosis and therapy. Expert Rev Neurother. 2009;9(6):835–46.
37. Niehaus L, Boelmans K. Diagnosis of Parkinson's disease–transcranial sonography in relation to MRI. Int Rev Neurobiol. 2010;90:63–79.
38. Sasaki M, Shibata E, Tohyama K, Takahashi J, Otsuka K, Tsuchiya K, et al. Neuromelanin magnetic resonance imaging of locus ceruleus and substantia nigra in Parkinson's disease. NeuroReport. 2006;17(11):1215–8.
39. •• Keren NI, Taheri S, Vazey EM, Morgan PS, Granholm AC, Aston-Jones GS, et al. Histologic validation of locus coeruleus MRI contrast in post-mortem tissue. Neuroimage. 2015;113(1):235–45. *This manuscript compares M-MRI hyperintense signal with histology and found neuromelanin containing neurons colocalize with hyperintense signal in NM-MRI images.*
40. Kitao S, Matsusue E, Fujii S, Miyoshi F, Kaminou T, Kato S, et al. Correlation between pathology and neuromelanin MR imaging in Parkinson's disease and dementia with Lewy bodies. Neuroradiology. 2013;55(8):947–53.
41. Bolding MS, Reid MA, Avsar KB, Roberts RC, Gamlin PD, Gawne TJ, et al. Magnetic transfer contrast accurately localizes substantia nigra confirmed by histology. Biol Psychiatry. 2013;73(3):289–94.
42. Dixon WT, Engels H, Castillo M, Sardashti M. Incidental magnetization transfer contrast in standard multislice imaging. Magn Reson Imaging. 1990;8(4):417–22.
43. Chen X, Huddleston DE, Langley J, Ahn S, Barnum CJ, Factor SA, et al. Simultaneous imaging of locus coeruleus and substantia nigra with a quantitative neuromelanin MRI approach. Magn Reson Imaging. 2014;32(10):1301–6.
44. Schwarz ST, Rittman T, Gontu V, Morgan PS, Bajaj N, Auer DP. T1-Weighted MRI shows stage-dependent substantia nigra signal loss in Parkinson's disease. Mov Disord. 2011;26(9):1633–8.
45. Trujillo P, Smith AK, Summers PE, Mainardi LM, Cerutti S, Smith SA, et al. High-resolution quantitative imaging of the substantia nigra. Conf Proc IEEE Eng Med Biol Soc. 2015;2015:5428–31.
46. Trujillo P, Summers PE, Ferrari E, Zucca FA, Sturini M, Mainardi LT, et al. Contrast mechanisms associated with neuromelanin-MRI. Magn Reson Med. 2017;78(5):1790–800.
47. Ogisu K, Kudo K, Sasaki M, Sakushima K, Yabe I, Sasaki H, et al. 3D neuromelanin-sensitive magnetic resonance imaging with semi-automated volume measurement of the substantia nigra pars compacta for diagnosis of Parkinson's disease. Neuroradiology. 2013;55(6):719–24.
48. Nakane T, Nihashi T, Kawai H, Naganawa S. Visualization of neuromelanin in the Substantia nigra and locus ceruleus at 1.5T using a 3D-gradient echo sequence with magnetization transfer contrast. Magn Reson Med. 2008;7(4):205–10.
49. Gorell JM, Ordidge RJ, Brown GG, Deniau JC, Buderer NM, Helpern JA. Increased iron-related MRI contrast in the substantia nigra in Parkinson's disease. Neurology. 1995;45(6):1138–43.
50. Haacke EM, Xu Y, Cheng Y-CN, Reichenbach JR. Susceptibility weighted imaging (SWI). Magn Reson Med. 2004;52:612–8.

51. de Rochefort L, Brown R, Prince MR, Wang Y. Quantitative MR susceptibility mapping using piece-wise constant regularized inversion of the magnetic field. Magn Reson Med. 2008;60(4):1003–9.
52. Li W, Wu B, Liu C. Quantitative susceptibility mapping of human brain reflects spatial variation in tissue composition. NeuroImage. 2011;55(4):1645–56.
53. Liu T, Spincemaille P, de Rochefort L, Kressler B, Wang Y. Calculation of susceptibility through multiple orientation sampling (COSMOS): a method for conditioning the inverse problem from measured magnetic field map to susceptibility source image in MRI. Magn Reson Med. 2009;61(1):196–204.
54. He N, Ling H, Ding B, Huang J, Zhang Y, Zhang Z, et al. Region-specific disturbed iron distribution in early idiopathic Parkinson's disease measured by quantitative susceptibility mapping. Hum Brain Mapp. 2015;36(11):4407–20.
55. Langkammer C, Schweser F, Krebs N, Deistung A, Goessler W, Scheurer E, et al. Quantitative susceptibility mapping (QSM) as a means to measure brain iron? A post mortem validation study. Neuroimage. 2012;62(3):1593–9.
56. Sun H, Walsh AJ, Lebel RM, Blevins G, Catz I, Lu JQ, et al. Validation of quantitative susceptibility mapping with Perls' iron staining for subcortical gray matter. Neuroimage. 2015;105:486–92.
57. Zheng W, Nichol H, Liu S, Cheng YC, Haacke EM. Measuring iron in the brain using quantitative susceptibility mapping and X-ray fluorescence imaging. Neuroimage. 2013;78:68–74.
58. House MJ, St Pierre TG, Kowdley KV, Montine T, Connor J, Beard J, et al. Correlation of proton transverse relaxation rates (R2) with iron concentrations in postmortem brain tissue from alzheimer's disease patients. Magn Reson Med. 2007;57(1):172–80.
59. Deistung A, Schafer A, Schweser F, Biedermann U, Turner R, Reichenbach JR. Toward in vivo histology: a comparison of quantitative susceptibility mapping (QSM) with magnitude-, phase-, and R2*-imaging at ultra-high magnetic field strength. Neuroimage. 2013;65:299–314.
60. Usunoff KG, Itzev DE, Ovtscharoff WA, Marani E. Neuromelanin in the human brain: a review and atlas of pigmented cells in the substantia nigra. Arch Physiol Biochem. 2002;110(4):257–369.
61. Langley J, Huddleston DE, Chen X, Sedlacik J, Zachariah N, Hu X. A multicontrast approach for comprehensive imaging of substantia nigra. Neuroimage. 2015;112:7–13.
62. Gramsch C, Reuter I, Kraff O, Quick HH, Tanislav C, Roessler F, et al. Nigrosome 1 visibility at susceptibility weighted 7T MRI-A dependable diagnostic marker for Parkinson's disease or merely an inconsistent, age-dependent imaging finding? PLoS ONE. 2017;12(10):e0185489.
63. Blazejewska AI, Schwarz ST, Pitiot A, Stephenson MC, Lowe J, Bajaj N, et al. Visualization of nigrosome 1 and its loss in PD: pathoanatomical correlation and in vivo 7 T MRI. Neurology. 2013;81(6):534–40.
64. Massey LA, Miranda MA, Al-Helli O, Parkes HG, Thornton JS, So PW, et al. 9.4 T MR microscopy of the substantia nigra with pathological validation in controls and disease. Neuroimage Clin. 2017;13:154–63.
65. Ohtsuka C, Sasaki M, Konno K, Koide M, Kato K, Takahashi J, et al. Changes in substantia nigra and locus coeruleus in patients with early-stage Parkinson's disease using neuromelanin-sensitive MR imaging. Neurosci Lett. 2013;541:93–8.
66. Matsuura K, Maeda M, Tabei KI, Umino M, Kajikawa H, Satoh M, et al. A longitudinal study of neuromelanin-sensitive magnetic resonance imaging in Parkinson's disease. Neurosci Lett. 2016;633:112–7.
67. Castellanos G, Fernandez-Seara MA, Lorenzo-Betancor O, Ortega-Cubero S, Puigvert M, Uranga J, et al. Automated Neuromelanin Imaging as a Diagnostic Biomarker for Parkinson's disease. Mov Disord. 2015;30(7):945–52.
68. Reimao S, Pita Lobo P, Neutel D, Correia Guedes L, Coelho M, Rosa MM, et al. Substantia nigra neuromelanin magnetic resonance imaging in de novo Parkinson's disease patients. Eur J Neurol. 2015;22(3):540–6.
69. Kashihara K, Shinya T, Higaki F. Neuromelanin magnetic resonance imaging of nigral volume loss in patients with Parkinson's disease. J Clin Neurosci. 2011;18(8):1093–6.
70. Schwarz ST, Xing Y, Tomar P, Bajaj N, Auer DP. In vivo assessment of brainstem depigmentation in parkinson disease: potential as a severity marker for multicenter studies. Radiology. 2017;283(3):789–98.
71. Isaias IU, Trujillo P, Summers P, Marotta G, Mainardi L, Pezzoli G, et al. Neuromelanin imaging and dopaminergic loss in Parkinson's disease. Front Aging Neurosci. 2016;8:196.
72. Reimao S, Pita Lobo P, Neutel D, Guedes LC, Coelho M, Rosa MM, et al. Substantia nigra neuromelanin-MR imaging differentiates essential tremor from Parkinson's disease. Mov Disord. 2015;30(7):953–9.
73. Kashihara K, Shinya T, Higaki F. Reduction of neuromelanin-positive nigral volume in patients with MSA, PSP and CBD. Intern Med. 2011;50(16):1683–7.
74. Ohtsuka C, Sasaki M, Konno K, Kato K, Takahashi J, Yamashita F, et al. Differentiation of early-stage parkinsonisms using neuromelanin-sensitive magnetic resonance imaging. Parkinsonism Relat Disord. 2014;20(7):755–60.
75. Miyoshi F, Ogawa T, Kitao SI, Kitayama M, Shinohara Y, Takasugi M, et al. Evaluation of Parkinson disease and Alzheimer disease with the use of neuromelanin MR imaging and (123)I-metaiodobenzylguanidine scintigraphy. AJNR. 2013;34(11):2113–8.
76. Wypijewska A, Galazka-Friedman J, Bauminger ER, Wszolek ZK, Schweitzer KJ, Dickson DW, et al. Iron and reactive oxygen species activity in parkinsonian substantia nigra. Parkinsonism Relat Disord. 2010;16(5):329–33.
77. Baudrexel S, Nurnberger L, Rub U, Seifried C, Klein JC, Deller T, et al. Quantitative mapping of T1 and T2* discloses nigral and brainstem pathology in early Parkinson's disease. Neuroimage. 2010;51(2):512–20.
78. Du G, Lewis MM, Styner M, Shaffer ML, Sen S, Yang QX, et al. Combined R2* and diffusion tensor imaging changes in the substantia nigra in Parkinson's disease. Mov Disord. 2011;26(9):1627–32.
79. Graham JM, Paley MN, Grunewald RA, Hoggard N, Griffiths PD. Brain iron deposition in Parkinson's disease imaged using the PRIME magnetic resonance sequence. Brain. 2000;123(Pt 12):2423–31.
80. Kosta P, Argyropoulou MI, Markoula S, Konitsiotis S. MRI evaluation of the basal ganglia size and iron content in patients with Parkinson's disease. J Neurol. 2006;253(1):26–32.
81. Martin WR, Wieler M, Gee M. Midbrain iron content in early Parkinson disease: a potential biomarker of disease status. Neurology. 2008;70(16 Pt 2):1411–7.
82. Peran P, Cherubini A, Assogna F, Piras F, Quattrocchi C, Peppe A, et al. Magnetic resonance imaging markers of Parkinson's disease nigrostriatal signature. Brain. 2010;133(11):3423–33.
83. Wallis LI, Paley MN, Graham JM, Grunewald RA, Wignall EL, Joy HM, et al. MRI assessment of basal ganglia iron deposition in Parkinson's disease. J Magn Reson Imaging. 2008;28(5):1061–7.
84. Aquino D, Contarino V, Albanese A, Minati L, Farina L, Grisoli M, et al. Substantia nigra in Parkinson's disease: a multimodal

MRI comparison between early and advanced stages of the disease. Neurol Sci. 2014;35(5):753–8.
85. Focke NK, Helms G, Pantel PM, Scheewe S, Knauth M, Bachmann CG, et al. Differentiation of typical and atypical Parkinson syndromes by quantitative MR imaging. AJNR. 2011;32(11):2087–92.
86. Mondino F, Filippi P, Magliola U, Duca S. Magnetic resonance relaxometry in Parkinson's disease. Neurol Sci. 2002;23(Suppl 2):S87–8.
87. Vymazal J, Righini A, Brooks RA, Canesi M, Mariani C, Leonardi M, et al. T1 and T2 in the brain of healthy subjects, patients with Parkinson disease, and patients with multiple system atrophy: relation to iron content. Radiology. 1999;211(2):489–95.
88. Ordidge RJ, Gorell JM, Deniau JC, Knight RA, Helpern JA. Assessment of relative brain iron concentrations using T2-weighted and T2*-weighted MRI at 3 Tesla. Magn Reson Med. 1994;32(3):335–41.
89. Gupta D, Saini J, Kesavadas C, Sarma PS, Kishore A. Utility of susceptibility-weighted MRI in differentiating Parkinson's disease and atypical parkinsonism. Neuroradiology. 2010;52(12):1087–94.
90. Dashtipour K, Liu M, Kani C, Dalaie P, Obenaus A, Simmons D, et al. Iron Accumulation Is Not Homogenous among Patients with Parkinson's disease. Parkinson's Dis. 2015;2015:324843.
91. Haller S, Badoud S, Nguyen D, Barnaure I, Montandon ML, Lovblad KO, et al. Differentiation between Parkinson disease and other forms of Parkinsonism using support vector machine analysis of susceptibility-weighted imaging (SWI): initial results. Eur Radiol. 2013;23(1):12–9.
92. Lotfipour AK, Wharton S, Schwarz ST, Gontu V, Schafer A, Peters AM, et al. High resolution magnetic susceptibility mapping of the substantia nigra in Parkinson's disease. J Magn Reson Imaging. 2012;35(1):48–55.
93. Lim IA, Faria AV, Li X, Hsu JT, Airan RD, Mori S, et al. Human brain atlas for automated region of interest selection in quantitative susceptibility mapping: application to determine iron content in deep gray matter structures. NeuroImage. 2013;82:449–69.
94. Lim IA, Li X, Jones CK, Farrell JA, Vikram DS, van Zijl PC. Quantitative magnetic susceptibility mapping without phase unwrapping using WASSR. NeuroImage. 2014;86:265–79.
95. Ryvlin P, Broussolle E, Piollet H, Viallet F, Khalfallah Y, Chazot G. Magnetic resonance imaging evidence of decreased putamenal iron content in idiopathic Parkinson's disease. Arch Neurol. 1995;52(6):583–8.
96. Ulla M, Bonny JM, Ouchchane L, Rieu I, Claise B, Durif F. Is R2* a new MRI biomarker for the progression of Parkinson's disease? A longitudinal follow-up. PLoS ONE. 2013;8(3):e57904.
97. Langley J, Huddleston DE, Sedlacik J, Boelmans K, Hu XP. Parkinson's disease-related increase of T2*-weighted hypointensity in substantia nigra pars compacta. Mov Disord. 2017;32(3):441–9.
98. • Huddleston DE, Langley J, Sedlacik J, Boelmans K, Factor SA, Hu XP. In vivo detection of lateral-ventral tier nigral degeneration in Parkinson's disease. Hum Brain Mapp. 2017;38(5):2627–34. *Histology findings of the substantia nigra in Parkinson's disease show selective loss of melanized dopamine neurons in the lateral-ventral SNc. This work provides the first direct imaging evidence showing a reduction of neuromelanin-sensitive signal in lateral-ventral tier of substantia nigra.*
99. German DC, Manaye K, Smith WK, Woodward DJ, Saper CB. Midbrain dopaminergic cell loss in Parkinson's disease: computer visualization. Ann Neurol. 1989;26(4):507–14.
100. Hassler R. Zur Pathologie der Paralysis agitains und des postenzephalitischen Parkinsonismus. J Psychol Neurol. 1938;48:387–476.
101. Schwarz ST, Afzal M, Morgan PS, Bajaj N, Gowland PA, Auer DP. The 'swallow tail' appearance of the healthy nigrosome—a new accurate test of Parkinson's disease: a case-control and retrospective cross-sectional MRI study at 3T. PLoS ONE. 2014;9(4):e93814.
102. Fu KA, Nathan R, Dinov ID, Li J, Toga AW. T2-imaging changes in the nigrosome-1 relate to clinical measures of Parkinson's disease. Front Neurol. 2016;7:174.
103. Mahlknecht P, Krismer F, Poewe W, Seppi K. Meta-analysis of dorsolateral nigral hyperintensity on magnetic resonance imaging as a marker for Parkinson's disease. Mov Disord. 2017;32(4):619–23.
104. Meijer FJ, Steens SC, van Rumund A, van Cappellen, van Walsum AM, Kusters B, Esselink RA, et al. Nigrosome-1 on susceptibility weighted imaging to differentiate Parkinson's disease from atypical parkinsonism: an in vivo and ex vivo pilot study. Pol J Radiol. 2016;81:363–9.
105. Schmidt MA, Engelhorn T, Marxreiter F, Winkler J, Lang S, Kloska S, et al. Ultra high-field SWI of the substantia nigra at 7T: reliability and consistency of the swallow-tail sign. BMC Neurol. 2017;17(1):194.
106. Reimao S, Ferreira S, Nunes RG, Pita Lobo P, Neutel D, Abreu D, et al. Magnetic resonance correlation of iron content with neuromelanin in the substantia nigra of early-stage Parkinson's disease. Eur J Neurol. 2016;23(2):368–74.
107. Blain CR, Barker GJ, Jarosz JM, Coyle NA, Landau S, Brown RG, et al. Measuring brain stem and cerebellar damage in parkinsonian syndromes using diffusion tensor MRI. Neurology. 2006;67(12):2199–205.
108. Schocke MF, Seppi K, Esterhammer R, Kremser C, Jaschke W, Poewe W, et al. Diffusion-weighted MRI differentiates the Parkinson variant of multiple system atrophy from PD. Neurology. 2002;58(4):575–80.
109. Langley J, Huddleston DE, Merritt M, Chen X, McMurray R, Silver M, et al. Diffusion tensor imaging of the substantia nigra in Parkinson's disease revisited. Hum Brain Mapp. 2016;37(7):2547–56.
110. Chan LL, Rumpel H, Yap K, Lee E, Loo HV, Ho GL, et al. Case control study of diffusion tensor imaging in Parkinson's disease. J Neurol Neurosurg Psychiatry. 2007;78(12):1383–6.
111. Vaillancourt DE, Spraker MB, Prodoehl J, Abraham I, Corcos DM, Zhou XJ, et al. High-resolution diffusion tensor imaging in the substantia nigra of de novo Parkinson disease. Neurology. 2009;72(16):1378–84.
112. Wang JJ, Lin WY, Lu CS, Weng YH, Ng SH, Wang CH, et al. Parkinson disease: diagnostic utility of diffusion kurtosis imaging. Radiology. 2011;261(1):210–7.
113. Menke RA, Scholz J, Miller KL, Deoni S, Jbabdi S, Matthews PM, et al. MRI characteristics of the substantia nigra in Parkinson's disease: a combined quantitative T1 and DTI study. NeuroImage. 2009;47(2):435–41.
114. Schwarz ST, Abaei M, Gontu V, Morgan PS, Bajaj N, Auer DP. Diffusion tensor imaging of nigral degeneration in Parkinson's disease: a region-of-interest and voxel-based study at 3 T and systematic review with meta-analysis. Neuroimage Clin. 2013;3:481–8.
115. Ziegler E, Rouillard M, Andre E, Coolen T, Stender J, Balteau E, et al. Mapping track density changes in nigrostriatal and extranigral pathways in Parkinson's disease. Neuroimage. 2014;99:498–508.
116. Fujiwara S, Uhrig L, Amadon A, Jarraya B, Le Bihan D. Quantification of iron in the non-human primate brain with

diffusion-weighted magnetic resonance imaging. Neuroimage. 2014;102(2):789–97.
117. Kamagata K, Hatano T, Okuzumi A, Motoi Y, Abe O, Shimoji K, et al. Neurite orientation dispersion and density imaging in the substantia nigra in idiopathic Parkinson disease. Eur Radiol. 2016;26(8):2567–77.
118. Ofori E, Pasternak O, Planetta PJ, Burciu R, Snyder A, Febo M, et al. Increased free water in the substantia nigra of Parkinson's disease: a single-site and multi-site study. Neurobiol Aging. 2015;36(2):1097–104.
119. Theisen F, Leda R, Pozorski V, Oh JM, Adluru N, Wong R, et al. Evaluation of striatonigral connectivity using probabilistic tractography in Parkinson's disease. Neuroimage Clin. 2017;16:557–63.
120. Kim M, Park H. Structural connectivity profile of scans without evidence of dopaminergic deficit (SWEDD) patients compared to normal controls and Parkinson's disease patients. Springerplus. 2016;5(1):1421.
121. Yoshikawa K, Nakata Y, Yamada K, Nakagawa M. Early pathological changes in the parkinsonian brain demonstrated by diffusion tensor MRI. J Neurol Neurosurg Psychiatry. 2004;75(3):481–4.
122. Goetz CG, Tilley BC, Shaftman SR, Stebbins GT, Fahn S, Martinez-Martin P, et al. Movement Disorder Society-sponsored revision of the Unified Parkinson's disease Rating Scale (MDS-UPDRS): scale presentation and clinimetric testing results. Mov Disord. 2008;23(15):2129–70.
123. Zhang Y, Wu IW, Buckley S, Coffey CS, Foster E, Mendick S, et al. Diffusion tensor imaging of the nigrostriatal fibers in Parkinson's disease. Mov Disord. 2015;30(9):1229–36.
124. Menke RA, Jbabdi S, Miller KL, Matthews PM, Zarei M. Connectivity-based segmentation of the substantia nigra in human and its implications in Parkinson's disease. NeuroImage. 2010;52(4):1175–80.
125. Marras C, Rochon P, Lang AE. Predicting motor decline and disability in Parkinson disease: a systematic review. Arch Neurol. 2002;59(11):1724–8.
126. Thenganatt MA, Jankovic J. Parkinson disease subtypes. JAMA Neurol. 2014;71(4):499–504.
127. von Coelln R, Shulman LM. Clinical subtypes and genetic heterogeneity: of lumping and splitting in Parkinson disease. Curr Opin Neurol. 2016;29(6):727–34.
128. Espay AJ, Schwarzschild MA, Tanner CM, Fernandez HH, Simon DK, Leverenz JB, et al. Biomarker-driven phenotyping in Parkinson's disease: a translational missing link in disease-modifying clinical trials. Mov Disord. 2017;32(3):319–24.
129. Schillaci O, Chiaravalloti A, Pierantozzi M, Di Pietro B, Koch G, Bruni C, et al. Different patterns of nigrostriatal degeneration in tremor type versus the akinetic-rigid and mixed types of Parkinson's disease at the early stages: molecular imaging with 123I-FP-CIT SPECT. Int J Mol Med. 2011;28(5):881–6.
130. Helmich RC, Janssen MJ, Oyen WJ, Bloem BR, Toni I. Pallidal dysfunction drives a cerebellothalamic circuit into Parkinson tremor. Ann Neurol. 2011;69(2):269–81.
131. Lewis MM, Du G, Sen S, Kawaguchi A, Truong Y, Lee S, et al. Differential involvement of striato- and cerebello-thalamo-cortical pathways in tremor- and akinetic/rigid-predominant Parkinson's disease. Neuroscience. 2011;177:230–9.
132. Ni Z, Pinto AD, Lang AE, Chen R. Involvement of the cerebellothalamocortical pathway in Parkinson disease. Ann Neurol. 2010;68(6):816–24.
133. He N, Huang P, Ling H, Langley J, Liu C, Ding B, et al. Dentate nucleus iron deposition is a potential biomarker for tremor-dominant Parkinson's disease. NMR Biomed. 2017. https://doi.org/10.1002/nbm.3554.
134. Galazka-Friedman J, Bauminger ER, Friedman A, Barcikowska M, Hechel D, Nowik I. Iron in parkinsonian and control substantia nigra—a Mossbauer spectroscopy study. Mov Disord. 1996;11(1):8–16.
135. Uitti RJ, Rajput AH, Rozdilsky B, Bickis M, Wollin T, Yuen WK. Regional metal concentrations in Parkinson's disease, other chronic neurological diseases, and control brains. Can J Neurol Sci. 1989;16(3):310–4.
136. Becker G, Seufert J, Bogdahn U, Reichmann H, Reiners K. Degeneration of substantia nigra in chronic Parkinson's disease visualized by transcranial color-coded real-time sonography. Neurology. 1995;45(1):182–4.
137. Guiney SJ, Adlard PA, Bush AI, Finkelstein DI, Ayton S. Ferroptosis and cell death mechanisms in Parkinson's disease. Neurochem Int. 2017;104:34–48.
138. Braak H, Tredici KD, Rüb U, de Vos RAI, Jansen Steur ENH, Braak E. Staging of brain pathology related to sporadic Parkinson's disease. Neurobiol Aging. 2003;24(2):197–211.
139. Zarow C, Lyness SA, Mortimer JA, Chui HC. Neuronal loss is greater in the locus coeruleus than nucleus basalis and substantia nigra in Alzheimer and Parkinson diseases. Arch Neurol. 2003;60(3):337–41.
140. Benarroch EE. The locus ceruleus norepinephrine system: functional organization and potential clinical significance. Neurology. 2009;73(20):1699–704.
141. Burke RE, Dauer WT, Vonsattel JPG. A critical evaluation of the Braak staging scheme for Parkinson's disease. Ann Neurol. 2008;64(5):485–91.
142. Jellinger K. A critical reappraisal of current staging of Lewy-related pathology in human brain. Acta Neuropathol. 2008;116(1):1–16.
143. Langley J, Huddleston DE, Liu CJ, Hu X. Reproducibility of locus coeruleus and substantia nigra imaging with neuromelanin sensitive MRI. MAGMA. 2017;30(2):121–5.
144. Kaasinen V, Vahlberg T. Striatal dopamine in Parkinson disease: a meta-analysis of imaging studies. Ann Neurol. 2017;82(6):873–82.
145. Kuya K, Ogawa T, Shinohara Y, Ishibashi M, Fujii S, Mukuda N, et al. Evaluation of Parkinson's disease by neuromelanin-sensitive magnetic resonance imaging and (123)I-FP-CIT SPECT. Acta Radiol. 2017. https://doi.org/10.1177/0284185117722812.